WORLD CONFERENCE ON TIMBER ENGINEERING 2025
BRISBANE, AUSTRALIA

Advancing Timber for the Future Built Environment

A NEW NODE-FOCUSED EXPERIMENTAL APPROACH TO INVESTIGATE LOAD-BEARING BEHAVIOR IN TIMBER TRUSSES

Lisa Stimpfle[1], Jan L. Wenker[2], Simon Aicher[3], Gerhard Dill-Langer[4]

ABSTRACT: To investigate the complex load-bearing behavior of timber trusses, particularly at the nodes, tests of complete trusses or partial sections of trusses would be necessary. However, these tests require a significant effort. Therefore, a new test method was developed to examine individual nodes, focusing on the most stressed ones. A test setup was designed to generate the internal force and moment ratios found in real trusses. It allows for variations in the connection angles of the individual members with manageable effort. Additionally, it enables adjustments regarding ratios of internal forces and moments of the components in order to investigate the effects of moment loadings in trusses that deviate from ideal frameworks. Consequently, the numerous varying parameters enable a comprehensive analysis of the load-bearing behavior of a truss joint while significantly reducing the effort compared to commonly used methods.

KEYWORDS: glulam timber truss, truss joint, multiaxial testing, bonded connections

1 – INTRODUCTION

Truss-like systems represent an efficient design approach characterized by optimized material usage and enhanced structural stiffness, particularly for wide-span constructions, where a significant amount of material can be saved compared to solid beams. In the joints connecting diagonals and chords, trusses show a complex load-bearing behavior, involving a combination of tension and compressive forces in the nodes, as well as stresses perpendicular to grain. The load-bearing capacity of trusses is usually determined by the most stressed node, located primarily in the peripheral area.

To understand the complex load-behavior of joint connections in trusses, uniaxial test are often insufficient, as the interaction of forces is not well represented compared to real trusses. While full-scale tests of complete trusses would provide the actual ratio of internal forces in real structures, the high costs associated with this method usually render this approach impractical.

In test methods for trusses, it is essential to consider the influence of the different load components acting on each node. This is particularly important for optimized truss structures with variable geometric parameters, such as cross-section heights of diagonals and connection angles.

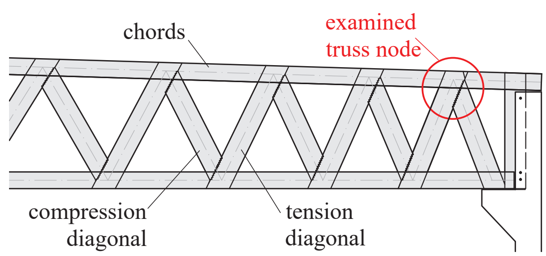

Figure 1: Illustration of the studied node within a truss

2 – BACKGROUND

There are several approaches for testing truss connections, mainly focusing on partial sections of trusses. Kobel et al. [7] described a three-point-bending test on short truss structures to verify the results of previous connection tests on dowel-type connections. The full-scale tests aimed to confirm the results of individual connection and embedment tests and to further examine the ductile behavior of the connections at a structural level.

Only a few approaches focus on the testing of individual truss nodes. Gehri [5] developed a test setup consisting of a truss node with a chord, a tension and a compression diagonal (see Fig. 2). Tensile loads are applied using a cylinder integrated into the testing platform. The compressive support of the chord and the compression diagonal generate compressive forces when the tensile load is introduced. However, due to the integrated cylinder, this test method is bound to special test equipment.

Meyer et al. [8] developed a full-size test method based on a test method for determining the shear strength of solid and glued laminated timber in EN 408 [4]. As normal forces in the diagonals result from shear between the upper and lower chords, the latter method introduces normal forces into these chords, thereby generating the necessary diagonal forces. This is realized by a compression test of a

[1] Lisa Stimpfle, Materials Testing Institute (MPA), University of Stuttgart lisa.stimpfle@mpa.uni-stuttgart.de
[2] Jan L. Wenker, Sustainability & Innovation, Brüninghoff Group, Heiden, Germany, jan.wenker@brueninghoff.de
[3] Simon Aicher, Materials Testing Institute (MPA), University of Stuttgart simon.aicher@mpa.uni-stuttgart.de
[4] Gerhard Dill-Langer, Materials Testing Institute (MPA), University of Stuttgart gerhard.dill-langer@mpa.uni-stuttgart.de

https://doi.org/10.52202/080513-0557

Figure 2: Test setup for truss nodes according to Gehri [5]

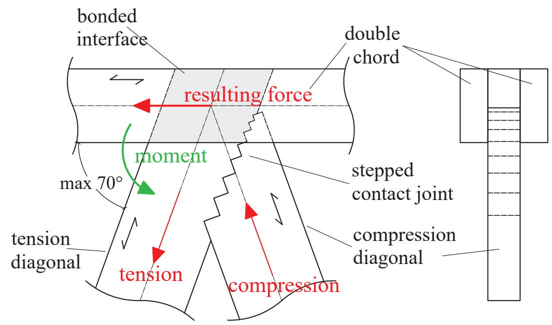

Figure 4: Design of the truss node with the decisive section forces and moments

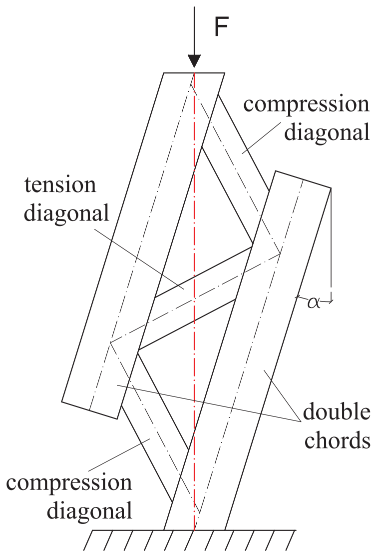

Figure 3: Testing method according to Meyer et al. [8]

truss section including four nodes (see Fig. 3) introducing the compressive forces directly in the chords. To avoid horizontal bearing forces the specimen is rotated by an angle α. The occurring internal forces can be compared to those of a real truss with exception to nodes at the tension chord, as only compressive loads are applied to the chords. As the compressive forces are not introduced parallel to the grain, the chords and especially the load introduction and support area must be adequately dimensioned. Additionally, the offset between the center of the load and the intersection of the system lines should be minimized to reduce resulting moments. Although this effect can be neglected for smaller dimensions, it has a significant influence on the detailing of the load introduction for larger components. The occurring internal forces primarily result from the geometry of the specimen, which is based on the truss geometry. Therefore, a deliberate variation of the ratio of internal forces and moments in individual components is not feasible with these tests.

3 – NEW TEST METHOD

3.1 PROJECT DESCRIPTION

The test method developed was conceived as part of a research project by the company Brüninghoff Group, Heiden, together with the MPA, University of Stuttgart, to develop a truss-like lightweight construction with both bonded and contact joints. The truss consists of two twin chord with bonded tension diagonals in between. The compression diagonals are connected to the tension diagonals through a specially stepped contact joint (see Fig.4). This ensures that the acting forces of the individual elements intersect at a single point in the node, thus reducing internal moments due to eccentricities – provided that the double chord is considered as a single system axis. All components are made from glued laminated timber (GLT), with the option of laminated veneer lumber (GLVL) in case of higher loads in the tension diagonals. The concept of the innovative construction is described in detail in [10].

As the investigated truss joint consists of a bonded interface between chords and tension diagonals, it deviates significantly from an ideal framework, as moments are also transferred by the bonded interfaces. These moments induce torsional stresses within the bonded interface. Additionally, shear stresses occur in the interface due to the resulting force induced by the coupling of the forces in the diagonals. Due to the counteracting forces in the diagonals with nearly equal values, the resulting force primarily acts along the grain direction of the chords (see Fig.4). The occurring moments and forces induce an interaction between torsional and shear stresses in the bonded interface, a phenomenon that requires detailed investigation in the ongoing project. It is essential to also consider the rotation direction, as reversed loads are also possible for load cases like wind uplift.

For the presented study the load-bearing capacity of the most stressed node was examined. For the studied truss this node is located at the outermost position on the upper (compression) chord as shown in Fig. 1. Consequently, a full-scale test setup for individual nodes, representing a realistic load distribution between the individual components, was developed. The specimens tested consist of tension and compression diagonals, as well as a part of the chord under

https://doi.org/10.52202/080513-0557

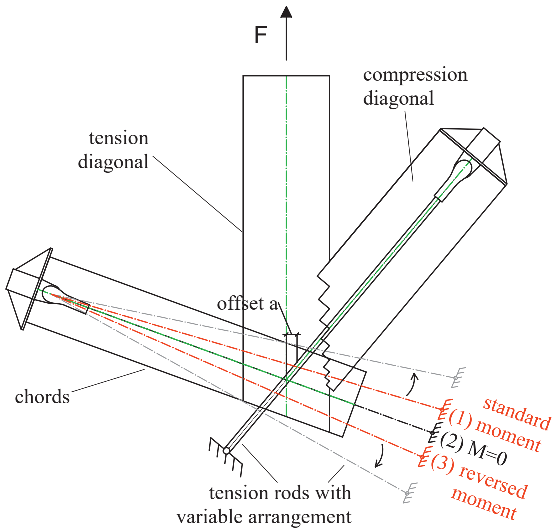

Figure 5: Geometry, application of loads and boundary conditions for the experimental test setup with possible variations

Figure 6: Realized test setup, i.e. series (2) - without moment loading (M=0)

compression. Especially for bonded connections full-scale testing of the geometry of the interface is necessary, as the load-bearing capacity decisively depends on stress peaks in the periphery of the bonded interface and on the size of the bonded faces.

3.2 EXPERIMENTAL SETUP

The developed test setup, illustrated in Fig. 5, anchors the twin chord and compression diagonal with tension steel rods aligned with their respective system lines. This design ensures pure compressive forces in the anchored components when a tensile force is applied in the tension diagonal, thereby creating a quasi-triaxial testing method. The steel rods are connected moment-free at both ends, avoiding the occurrence of additional internal forces. The anchor point of the steel rods can be varied to allow for an adjustable connection angle of the joint components.

Furthermore, an additional internal moment in the joint can be induced by applying an offset a between the intersection point of the system lines of the cross-sections and the intersection point of the steel rods (see Fig. 5). This is realized by varying the anchoring position of the chord's steel rods. By means of different offsets, deliberately chosen additional moment loads can be applied. One realized test setup is shown in Fig. 6

The experimental setup allows for variations in both, the geometry of the truss node and the ratio of the moment loading. In contrast to the above mentioned testing methods in literature, the adjustable positioning allows for the variation of the moment-shear ratio in the joint, enabling a comprehensive analysis of the torsional behavior and its impact on the load-bearing capacity of the truss joint.

3.3 TEST CONFIGURATIONS

To represent the various requirements of a joint, such as the varying moment-shear ratio and different connection angels, a set of test series was performed.

The following setups were realized: series (1) with a small offset a corresponding approximately to the ratio between forces and moments of the outer node of a designed truss, (2) without applied moment loading ($a = 0$), (3) the same offset a and ratio between force and moments as in (1) with a reversed rotation direction. An overview of the test setups is given in Table 1. The test series without moment loading is used for the isolated investigation of a pure shear load in the bonded interface. The specified moment-force-ratio was defined based on the standard normal force-to-moment distribution at the most stressed outer truss node in the edge region, where this ratio was set to 1 in the following. In this context, the force is defined as the calculated axial force in the chord. The standard moment-force-ratio of 1 correspond to an offset of $a = 37\,\text{mm}$. Furthermore, the influence of the reversed moment direction, which can occur due to effects such as wind uplift, was also investigated and is defined by a moment-force-ratio of -1. Figure 5 shows the different possible setups.

There are several possible variations of the test setup, which could be tested in the future: Increasing the offset between the intersection point of the system lines of the cross-sections and the intersection point of the steel rods results in a higher moment contribution, thereby increasing the moment-force-ratio accordingly. This offers the possibility to analyse the load-bearing behavior of the bonded interface in detail, in particular the moment-shear interaction in the interface.

Additionally, test setups with altering angles between the chord and the diagonals can be examined to consider

Table 1: Overview of test series

description	enclosed fiber angle in bonded interface [°]	offset a [mm]	moment-force-ratio [-]
(1) standard moment loading	70	37	1
(2) without moment loading	70	0	0
(3) reversed standard moment loading	70	-37	-1

the varying angles along the length of the truss and in particular to investigate the influence of the bonding angle on the load-bearing capacity.

3.4 COMPARISON OF SECTION FORCES IN THE TRUSS AND IN THE NEW TEST METHOD

The correct load distribution of the test setup was ensured by means of numerical modeling comparing the test setup with a model of a complete truss. Both, the model of the complete truss and the different experimental configurations were studied with a simple framework model using the software RSTAB 8 [9].

The model of the complete truss was set with a length of 36 m and loaded with a uniform line load. The connection between chord and tension diagonal was modeled as a rigid joint due to the high stiffness of the adhesive bonding, while the contact connection of the compression diagonal was assumed to be moment-free.

The framework model of the new test method was set up based on the actual experimental test setup. The truss nodes, i.e. the intersection between the individual components were modeled identically to those of the truss model. The anchoring of the node was realized using appropriate boundary conditions and a load of 100 kN was applied at the end of the tension diagonal.

The internal forces and moments in the model of the new test method were compared with those in the outermost node in the compression chord of the truss model. (see Table 2). The loads in the complete truss were scaled so that the force in the tension diagonal corresponds to that of the test setup models. As the test series with standard moment loading (1) is meant to represent a truss node under a typical load distribution, these internal forces are compared in detail, to validate the correct load distribution of the designed test setup. The resulting internal moments and forces largely coincide. Although the forces in the compression diagonal of the truss are slightly higher, this difference is negligible in this context. More importantly, the forces in the chord, which correspond to the before mentioned resulting force from an interaction between the diagonals – responsible for the shear loading in the bonded connection – are more or less equal, as well as the occurring moments in the interface.

Further framework calculations show that the possible test setup variations with larger offsets – resulting in increased moment loading in the bonded interface – also exhibit increasing moments in that area, proportional to the size of the offset.

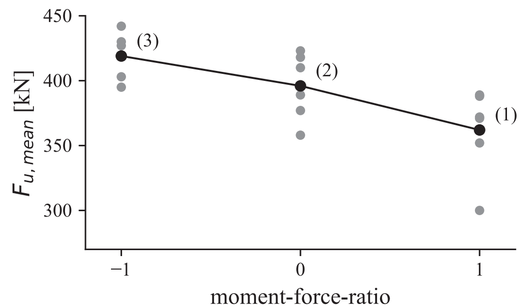

Figure 7: Mean failure loads $F_{u,mean}$ of the test series

These investigations demonstrate that the presented testing method provides a realistic approach to represent the load-bearing behavior of a truss node.

4 – EXPERIMENTAL RESULTS

The evaluation of the experimental results focuses on the series with GLVL in the tension diagonal and three different moment-force-ratios: the test series with standard moment loading (1), without moment loading (2) and with reversed standard moment (3). Each of these series was conducted with 5 or 6 specimens.

The results, including mean failure loads $F_{u,mean}$, coefficient of variation (COV) and the characteristic loads $F_{u,k}$ are presented in Table 3. Characteristic values are calculated according to EN 14358 [3] with the corresponding COV (min. 5%) and for a better comparability with an equal parameter k_s for a specimen number of 6. As there are two competing failure mechanisms – failure in the stepped contact joint or in the bonded interface – additionally the number of specimens failing in the bonded interface is specified.

Overall all specimens show a brittle behavior and exhibit an immediate load drop upon reaching the maximum load. In addition, some specimens show a slight non-linearity before reaching the maximum load.

The specimens revealed average failure loads of 362 kN, 396 kN and 419 kN for the tests with standard (1), without (2) and reversed moment loading (3), respectively. Starting from the series without moment loading (2) a decrease of the failure load of approx. 8.5 % is observed for a moment loading in the rotational direction corresponding to the real truss (1). With a moment loading in the opposite direction resulting from reversed loads (3), an increase of the failure load of approx. 5.8 % was reached. The COV ranging from

https://doi.org/10.52202/080513-0557

Table 2: Comparison of the calculated forces and moments obtained from models of complete truss and test setups

		complete truss	test setups (1)	(2)	(3)
moment-force-ratio	[-]	1.0	1.0	0	-1.0
force in the tension diagonal	[kN]	100	100	100	100
force in the compression diagonal	[kN]	114	102	100	98
force in the chord	[kN]	76	72	68	65
moments in the bonded interface	[kNm]	3.7	3.8	0	-3.6

5 % to 10 % proved a relatively small scatter of the test results.

In this test setup, two possible failure mechanisms could be observed: a failure of the stepped contact joint occurring as shear failure in the tension diagonal and a failure in the bonded interface or, more specifically, in the adjacent wooden areas next to the bonded interface. For the series without moment loading (2), one-third of the specimens failed in the bonded interface. In the series with standard moment loading (1), the number of specimens failing in the bonded interface increased. For both series the failure mechanism of the stepped contact joint and the bonded interface seem to compete at a rather similar load-bearing level. In contrast, under reversed moment loading, failure was governed by the stepped contact joint, as none of the specimens failed in the bonded connection. Obviously, for this series the load-bearing capacity of the bonded interface would be higher than the maximum loads of the tested specimens.

The resulting effective shear strength of the stepped contact joint can be determined in a simplified approach. For this purpose, the applied loads in the compression diagonal are derived based on the maximum loads and the framework model. Using angular relationships, the shear component of the force is then calculated. This shear force is compared to the contact surface of the stepped contact joint, which is approximated by the projected length of the stepped contact joint. The resulting average shear strengths are $\tau_v = 3.1\,\mathrm{N/mm^2}$, $3.5\,\mathrm{N/mm^2}$, and $3.6\,\mathrm{N/mm^2}$ for series (1), (2), and (3), respectively. The specified shear strengths partially represent minimum values in cases where failure occurred in the bonded interface.

The evaluation of the bonded joint is further examined using a modeling approach in the following.

Table 3: Compilation of test results

moment-force-ratio		(1) 1	(2) 0	(3) -1
number of specimens	[-]	6	6	5
$F_{u,mean}$	[kN]	362	396	419
COV	[%]	9.2	6.5	4.7
$F_{u,k}$	[kN]	284	336	370
failure in the bonded interface	[-]	4/6	2/6	0/5

4.1 POST-FAILURE INSPECTION OF THE SPECIMENS

In case of specimens where failure occurred in the stepped contact joint, cracks appear along the bottom of the steps. These cracks developed either within a single layer or across multiple, closely spaced layers, depending on the embedment depth of the steps. A representative failure pattern of the stepped contact joint is shown in Figs. 8 and 9.

In some cases, additional cracks parallel to the GLVL layers originating from the edge of the outermost top step, were observed. Those cracks are likely caused by stresses perpendicular to grain, as the outer steps act similarly as notches. As the cracks are observed already shortly before failure they could assumingly initiate the failure of the stepped contact joint. For some specimens, additional cracks parallel to the grain were detected in the compression diagonal. These cracks were likely initiated by the transfer of the non-linear deformations within the GLVL to the glulam counterpart by frictional locking causing stresses perpendicular to the grain.

In the series with reversed moment loading (3), no failure occurred in the bonded interface. The fracture surfaces in the bonded interface are exemplarily shown for a specimen of the series with standard (1) and without moment loading (2) in Fig.10. Inspection of the failed bonded areas showed a high wood fiber percentage, ranging from 90% to 100%. In both cases, failure primarily occurred in the tension diagonal, while failure in the chord was minimal. The wood fiber percentage were quantitatively analyzed for different regions within the bonded interface. The regions are labeled according to Fig.11

A difference in the wood fiber percentage in the chord was observed between the upper region near the stepped contact joint at position *A* (see Fig. 11) and the remaining areas. In the upper region near the stepped contact joint (position *A*), the percentage was very low (5–10%), whereas it was slightly higher in the other areas (10–19%). Series with standard moment loading (1) showed a slightly higher wood fiber percentage in the chord (15–19%) compared to the series without moment loading (10–15%).

5 – MODELLING

5.1 MODEL DESCRIPTION

To investigate the effect of the moment-shear ratio, the stress distribution within the bonded interface was analyzed

https://doi.org/10.52202/080513-0557

Figure 8: Representative failure in the stepped contact joint (series (1) – side view

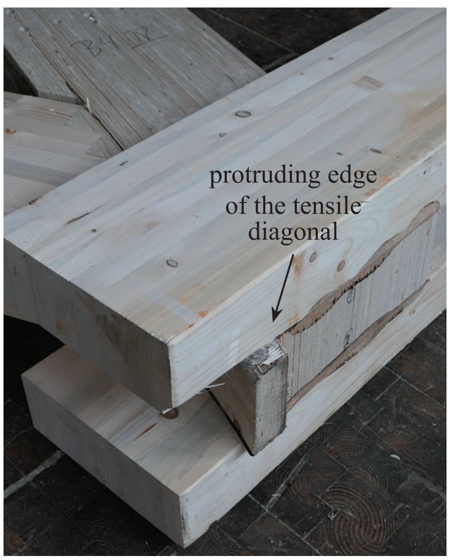

Figure 9: Representative failure in the stepped contact joint (series (2) – bottom view

using finite element (FE) calculations. This was performed by a 3D parametric finite element model representing the test setup using the commercial software Abaqus 2023 [1] via its Python API. The geometry and dimensions of the model are based on the test setup, consisting of a truss node with chord, tension and compression diagonal.

The model takes advantage of the symmetry in direction of the components' thickness. Consequently, both the tension and compression diagonal are reduced to half of the total thickness and one of the chords of the double-chord system could be omitted. Since the primary focus is on the investigation of the bonded interface, the geometry of the

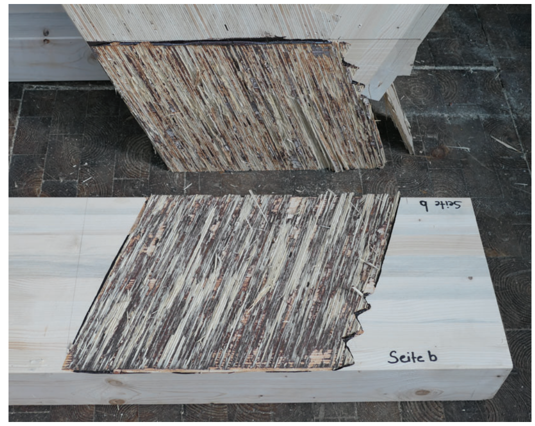

(a) specimen of series (2)

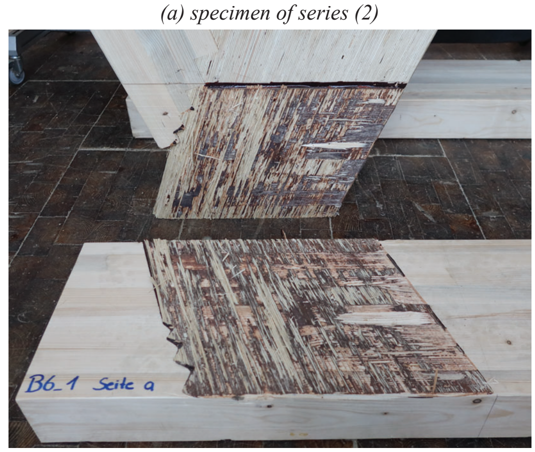

(b) specimen of series (1)

Figure 10: Representative fracture surfaces observed in the bonded interface

stepped contact joint is simplified.

The support conditions are realized by rigidly connected steel plates with high stiffness at the ends of chord and compression diagonal, which are attached to steel rods. The end points of the modelled steel rods are assumed as fixed in all three dimensions. The load of $F = 100\,\mathrm{kN}$ is applied at the top end of the tension diagonal.

Both, the connection between the chord and the tension diagonal in the bonded interface and the contact connection between the diagonals is modeled using "*Tie constraints*". For all components, except the rigid elements, linear 3D elements with reduced integration (C3D8R) with a size of about 10 mm were used. The material properties are defined according to [2] and [11] and are listed in Table 4.

Corresponding to the three experimental test series calculations for three different moment-force-ratios were performed: (1) with a standard moment loading, (2) without additional moment loading and (3) with a reversed standard moment loading of the same amount. The adjusted offsets between the intersection point of the system lines of the cross-sections and the intersection point of the steel rods correspond to those specified in Table 1. These offsets and the resulting moments in the bonded interface are deter-

https://doi.org/10.52202/080513-0557

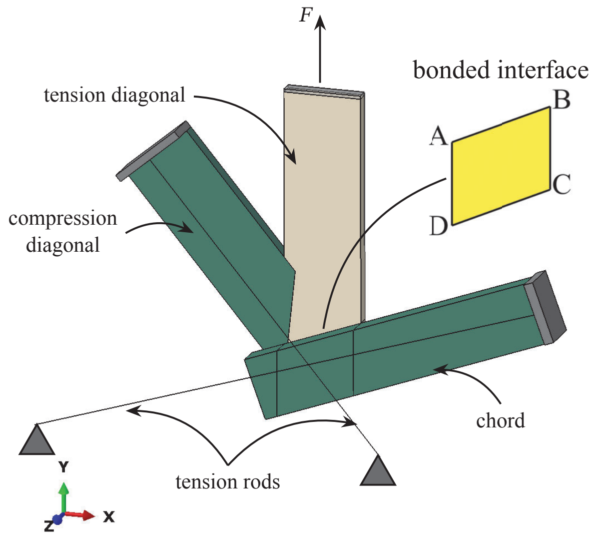

Figure 11: Geometry of the finite element model

mined by the position of the anchoring points of the rods. The geometry of the finite element model is exemplary shown in Fig. 11 for the standard moment loading (1).

5.2 RESULTS

For the evaluation of the load-bearing behavior of the bonded connection, the stress distribution in the bonded interface between tension diagonal and chords is examined in detail. The shape and position of the interface is sketched in Fig. 11. The results show the longitudinal $\tau_{v,0}$ and rolling shear $\tau_{v,90}$ stress distributions in the area of the bonded joint, separately for the respective sections in the tension diagonal and the chord. By comparing the models of the three series the influence of the direction of the moment can be examined in detail. The stress distibutions are shown in the contour plots in Fig. 12. The specified values correspond to an applied tensile load of 100 kN.

The labels used for the positions within the bonded interface are defined according to Fig.11. Position *A* is located on the upper side of the bonded interface, facing the stepped contact joint. Similarly, position *C* is also oriented toward the stepped contact joint but on the lower side. In contrast, position *B* is situated on the upper side, facing away from the stepped contact joint, while position *D* is on the lower side.

All plots show a pronounced uneven stress distribution, with maximum stresses occurring primarily within local stress concentration areas near the attached compression diagonal (position *A*). Additionally, for all stress components, the maximum stress increases when the moment acts in the standard direction (1) and decreases when the moment acts in the reversed direction (3), compared to tests without additional moment loading (2).

For the longitudinal shear stress in the tension diagonal, in addition to the localized stress concentrations near position *A*, standard moment loading induces further shear stresses — at a lower level — along the edge between positions *B* and *C*. For the rolling shear stress in the tension diagonal, the standard moment loading (1) results in higher but also more widely distributed rolling shear stresses. These stresses are concentrated primarily along the upper edge between positions *A* and *B* of the bonded interface, but also spread across the upper region with considerable stress levels (see Fig.12b). Due to the orientation of the tension diagonal and chord relative to each other (70 degrees), the rolling shear stresses in the tension diagonal corresponds qualitatively to the longitudinal shear stresses in the chord. The rolling shear stresses in the chord remain relatively low, except for a highly localized zone near position *A*.

The maximum stresses occurring in the bonded interface are compared between the three series in Fig. 13. For an estimation of the stresses occurring at failure, the stresses can be scaled by a factor of 3 to 4, depending on the maximum tensile force in the experiments.

The longitudinal and rolling shear stresses in both components increase around 8% with a moment acting in standard direction (1). For a reversed moment loading (3) longitudinal shear in both components and rolling shear in the tension diagonal decrease between 16% and 21%. Only the maximum rolling shear stress in the chord is increasing for reversed moment loading, indicating that this stress component is not decisive for the failure. This is a rather simplified approach, as the stress distributions are partially extremely inhomogeneous and stress concentrations are also dependent on the mesh of the finite element model. Especially for a comparison with strength values, an approach that accounts for a proper evaluation of the local stress concentrations (e.g. a Weibull stress concept [6]) would be necessary.

5.3 COMPARISON OF EXPERIMENTAL AND MODELLING RESULTS

Comparing the experimental and the modeling results in Figs. 7 and 13 a correlation between the maximum loads and the occurring stresses can be observed. This correlation is shown in Fig. 14. In cases where failure occurred in the bonded interface, the wood fiber percentage showed up mainly in the tension diagonal. Starting from the series without moment loading (2) the longitudinal and rolling

Table 4: Stiffness values used for the materials in the finite element models

Material	E_x [MPa]	E_y [MPa]	E_z [MPa]	ν_{xy} [–]	ν_{xz} [–]	ν_{yz} [–]	G_{xy} [MPa]	G_{xz} [MPa]	G_{yz} [MPa]
spruce GLT	11 500	300	300	0.02	0.02	0.2	650	650	65
spruce GLVL	13 800	430	430	0.02	0.02	0.2	600	600	60

https://doi.org/10.52202/080513-0557

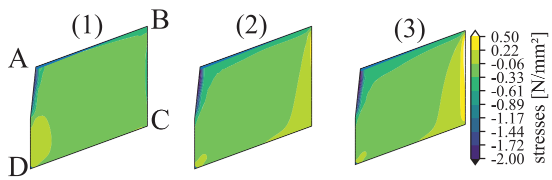

(a) longitudinal shear stresses $\tau_{v,0}$ on side of the tension diagonal

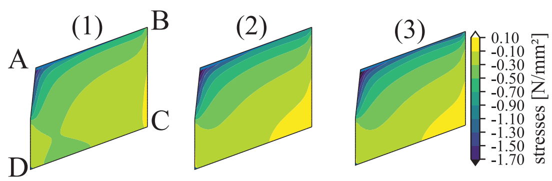

(b) rolling shear stresses $\tau_{v,90}$ on side of the tension diagonal

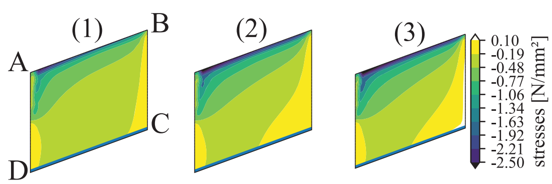

(c) longitudinal shear stresses $\tau_{v,0}$ on side of the chord

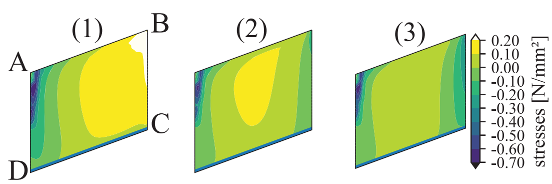

(d) rolling shear stresses $\tau_{tv,90}$ on side of the chord

Figure 12: Contour plots showing the stress distribution along the bonded interface for a total load of $F = 100kN$

shear stresses in the tension diagonal increase by approximately 7% to 8% for standard moment loading (1), and evidently lead to earlier failure of the specimens. This is comparable to the experimental results, as the maximum load of series (1) falls short of that of series (2) by approximately 9%. In the opposite moment direction (3), the stresses decrease by approximately 16% to 21% compared to moment-free series (2). The corresponding experimental results show an increase of the failure load of about 6%, which is significantly lower than the relative changes in the stresses. Since all specimens in this series failed in the stepped contact joint, obviously the load-bearing capacity of the bonded interface is not reached yet. It can be assumed that the interface capacity should exceed the failure load of the stepped contact joint by the amount of the maximum stress values.

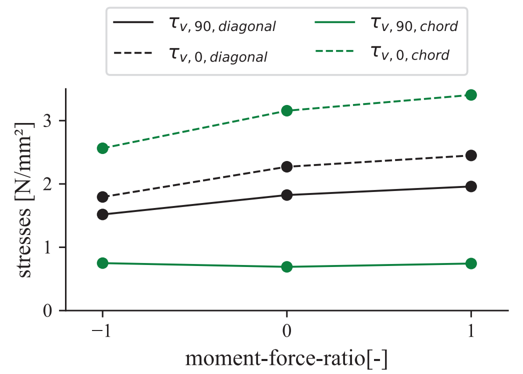

Figure 13: Maximum stresses in the bonded interface for a total load of $F = 100\,\text{kN}$

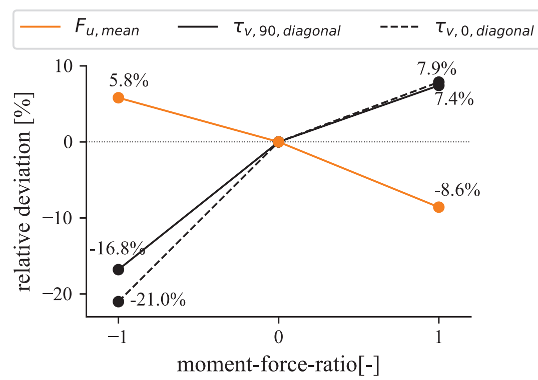

Figure 14: Relative deviations of the mean failure loads $F_{u,mean}$ and of longitudinal and rolling shear stresses in the tension diagonal depending on moment-force-ratios

6 – DISCUSSION

The comparison between the numerical models of the complete truss and the new test method showed an overall agreement of the internal forces and moments. Only the internal forces of the compression diagonal in the test setup deviate slightly. This can be neglected, as the decisive stress components are the force in the chord and the moment. Furthermore, additional investigations showed that by adjusting the anchoring positions, a variation in the moment loading and its influence on the bonded interface can be investigated.

Obviously, the rotational direction of the moment significantly influences the load-bearing capacity of the connection. This suggests that the stresses induced by shear forces and moments in the bonded interface lead to a stress superposition, which negatively impacts the load-bearing behavior under standard moment loading while having a beneficial effect in the reverse direction.

Qualitatively, the relative deviations in longitudinal and rolling shear stresses predict the relative failure loads quite well for all three series. For the series without (2) and with

https://doi.org/10.52202/080513-0557

standard moment loading (1) these deviations also align quantitatively. Furthermore, the predominant failure in the bonded interface on the side of the tension diagonal supports the assumption that longitudinal and rolling shear in this region are the decisive failure mechanisms. The interaction between these stress components requires further investigation.

Although the relative deviations between loads and the stresses fit qualitatively for reversed moment loading, the actual failure loads are lower than predicted by the stresses. This discrepancy can be explained by the exclusive failure in the stepped contact joint, which prevents the bonded interface from reaching its full load-bearing capacity.

7 – CONCLUSIONS AND OUTLOOK

The paper presents details on the development and the structure of the new test setup, investigating the joints of timber trusses and providing a comparison to other testing methods. The section force distribution of the presented test setup and a corresponding complete truss is compared in a modeling approach, showing that the new test method mirrors the real truss conditions very closely. Additionally, it enables a more detailed analysis of the influence of the moment direction and moment-force-ratio on the load-bearing capacity of the connection, especially for the investigated joint with rigidly bonded connections between tension diagonals and chords.

Furthermore, details of selected test series and the experimental results are presented, showing the influence of the moment direction on the load-bearing capacity of the joint. In the performed tests, rolling shear stress in the tension diagonal was identified as the decisive failure mechanism. However, the interaction between rolling shear and other stress components requires further investigation.

For future research, similar investigations will be performed for tension diagonals made of glued laminated timber (GLT). Moreover, the ability of the test setup to apply increased moment loading will be used to examine its effects on the load-bearing behavior of the bonded interface. Furthermore, the possible increase in moment in the realized test setup loading will be used to investigate its effects on the stress distribution within the bonded interface.

ACKNOWLEDGEMENTS

The close cooperation in the R&D project and the subsequent approval investigations with the company Brüninghoff Group, including PLANSITE part of the Brüninghoff Group, is gratefully acknowledged. All specimens and some part of the testing equipment (i.e. the special steel frame) were designed and developed jointly and have been produced and made available by the Brüninghoff Group.

REFERENCES

[1] Abaqus. *ABAQUS/Standard User's Manual, Version 2023*. Providence, RI, USA: Dassault Systèmes, 2023.

[2] EN 14080. *Timber structures – Glued laminated timber and glued solid timber – Requirements*. Brussels, Belgium: European Committee for Standardization, 2013.

[3] EN 14358. *Timber structures - Calculation and verification of characteristic values*. Brussels, Belgium: European Committee for Standardization, 2016.

[4] EN 408. *Timber structures – Structural timber and glued laminated timber – Determination of some physical and mechanical properties*. Brussels, Belgium: European Committee for Standardization, 2012.

[5] E. Gehri. "Performant connections – a must for veneer-based products." In: *Proceedings of the World Conference on Timber Engineering (WCTE 2018)*. Vienna: WCTE, 2016.

[6] L. Höfflin and S. Aicher. "Design of rectangular holes in glulam beams." In: *Otto-Graf-Journal* 14 (2003), pp. 211–229.

[7] P. Kobel, A. Frangi, and R. Steiger. "Timber trusses made of European Beech LVL." In: *Proceedings of the World Conference on Timber Engineering (WCTE 2016)*. Vienna: WCTE, 2016.

[8] N. Meyer and H. J. Blaß. "Eine neue Prüfmethode für Fachwerkknoten aus Holz." In: *Bautechnik* 95 (2018), pp. 793–800.

[9] RSTAB. *RSTAB 8*. Tiefenbach, Germany: Dlubal Software GmbH, 2018.

[10] J. Wenker, L. Schlüter, J. Schneermann, L. Stimpfle, G. Dill-Langer, and F. Steffens. "Glued wide-span timber trusses – a design and experimental approach." In: *Proceedings of the World Conference on Timber Engineering (WCTE 2025)*. Brisbane: WCTE, 2025.

[11] Z-9.1-847. *Bauarten mit Furnierschichtholz "Kerto LVL S-beam", "Kerto LVL Q-panel" und "Kerto LVL Qp-beam"*. Berlin, Germany: Deutsches Institut für Bautechnik, 2024.